



# Polystyrene@graphene oxide-Fe<sub>3</sub>O<sub>4</sub> as a novel and magnetically recyclable nanocatalyst for the efficient multi-component synthesis of spiro indene derivatives

Seyedeh Fatemeh Hojati<sup>1</sup> · Amirhassan Amiri<sup>1</sup> · Maryam Mahamed<sup>1</sup>

Received: 28 July 2019 / Accepted: 9 October 2019  
© Springer Nature B.V. 2019

## Abstract

Polystyrene (PS)-coated magnetic graphene oxide (GO-Fe<sub>3</sub>O<sub>4</sub>) nanocomposite has been prepared and characterized by FT-IR, TEM and VSM techniques, and its catalytic activity has been evaluated in the multi-component synthesis of two series of indene derivatives. The three-component condensation of ninhydrin/isatin, malononitrile and active methylene-containing compounds and also the four-component condensation of ninhydrin, *o*-phenylenediamines, malononitrile and active methylene-containing compounds were satisfactorily performed in the presence of PS@GO-Fe<sub>3</sub>O<sub>4</sub> magnetic nanocomposite, and corresponding 2'-aminospiro[indene-2,4'-pyran]-3'-carbonitriles, 2'-aminospiro[indoline-3, 4'-pyran]-3'-carbonitriles and 2'-aminospiro[indeno[1,2-*b*]quinoxaline-11,4'-pyrane]-3'-carbonitriles were obtained in good-to-excellent yields, respectively. Very shorter reaction times than the reported methods, easy workup procedure and easy separation and reusability of the catalyst are noteworthy advantages of the current method.

**Keywords** Spiro indene derivatives · One-pot synthesis · Polystyrene@GO-Fe<sub>3</sub>O<sub>4</sub> nanocomposite · Multi-component reaction

## Introduction

During the years, the synthesis of spiro-type compounds has attracted much interest as an important target in chemical synthesis because of their extensive biological activities [1–3]. The best method to get this goal is development of multi-component reactions (MCRs). Multi-component reactions are strong tools for the synthesis of multi-functional spiro heterocycles in which three or more reactants combine together in a one-pot reaction to form new products [4–7]. 4H-pyran derivatives have

✉ Seyedeh Fatemeh Hojati  
hojatee@yahoo.com; sf.hojati@hsu.ac.ir

<sup>1</sup> Department of Chemistry, Hakim Sabzevari University, Sabzevar 96179-76487, Iran

gained much attention due to their pharmaceutical and biological properties such as antiviral [8], anticancer [9], anticoagulant [10], antiallergic [11, 12], hypoglycemic and microbial effects [13]. These compounds have been known as key moieties in numerous biologically active natural products [14, 15]. Quinoxaline is another biologically active scaffold that antibacterial [16], antifungal [17], antidepressant [17] and antitumor [18] activities have been detected for its derivatives. On the other hand, more focus has been given to indene and indoline and spiro compounds of them for their pharmaceutical activities [19–22] such as anti-inflammatory [23], antibacterial [24], analgesic and antioxidant [24] properties. A quick and direct route to the synthesis of spiro[indene-2,4'-pyran]-3'-carbonitrile, spiro[indoline-3,4'-pyran]-3'-carbonitrile and 2'-aminospiro[indeno[1,2-*b*]quinoxaline-11,4'-pyran]-3'-carbonitriles is multi-component reaction. Several methods have been reported for the synthesis of these heterocycles, and most of them have some limitations such as long reaction times [25–27], requiring large amounts of the catalyst [28] and the use of toxic [28] or nonreusable reagent [26–28]. Therefore, development of a facile and economical synthetic route to spiro indene and spiro indoline derivatives is still in demand.

Graphene is a strong and thick honeycomb lattice system and has found extreme applications in composites [29, 30], transparent conducting films [31], sensors [32], supercapacitors [33], nanoelectronics [34], batteries [35], biotechnology [36] and catalyst supports [37, 38] because of its magical characteristics. The high surface area, flexibility, porous structure and thermal, chemical, mechanical and structural stability are valuable properties of graphene. Graphene oxide (GO) is an oxygenated form of graphene that is usually used as an efficient starting material for the preparation of nanocomposites [39, 40]. Loading magnetic nanoparticles such as Fe<sub>3</sub>O<sub>4</sub> on the surface of graphene oxide converts it into a magnetic nanocomposite [41]. Recently, different polymers have been widely used to coat magnetic nanoparticles [42]. In this study, the surface of magnetized graphene oxide was coated by a layer of polystyrene to increase the resistance of Fe<sub>3</sub>O<sub>4</sub> nanoparticles to oxidation and prevent the leaching of nanoparticles from the graphene oxide surface.

In the following of our previous works on the design and development of new catalytic system for the preparation of biologically active heterocycles [43–49], herein, we wish to report the preparation of a polystyrene-coated magnetic graphene oxide (PS@GO-Fe<sub>3</sub>O<sub>4</sub>) and its application in the synthesis of spiro indene and spiro indoline derivatives as a reusable and highly efficient catalyst. This magnetic nanocomposite was characterized by Fourier infrared spectroscopy (FT-IR), scanning electron microscopy (SEM) and vibrating sample magnetometry (VSM) analyses.

## Experimental section

### Materials and instruments

Chemicals were purchased from Merck Chemical Company. IR spectra were recorded on a Shimadzu FT-IR 8440 spectrophotometer. <sup>1</sup>H NMR spectra were recorded on a Bruker Avance 300 MHz spectrometer in deuterated DMSO. Melting

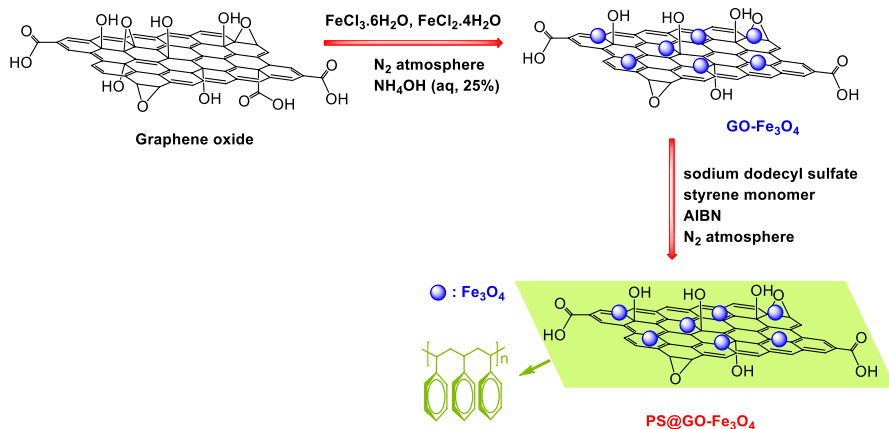
points were determined with electrothermal 9100 apparatus and were uncorrected. The morphology of PS@GO-Fe<sub>3</sub>O<sub>4</sub> and size of nanoparticles were determined by transmission electron microscopy (TEM) model Leo 1450 VP. The magnetic character of catalyst was evaluated by a vibrating sample magnetometer (Meghnatis Daghigh Kavir Corporation, Kashan Kavir; 114 Iran). Elemental analyses were performed using a Heraeus CHN-O-Rapid analyzer. Mass spectra were recorded on a VG micromass 7070H and Finnigan Mat 1020B mass spectrometers operating at 70 eV.

### Preparation of magnetic graphene oxide

Graphene oxide (GO) was prepared via modified Hummers' method from natural graphite [50]. A concentrated mixture of H<sub>2</sub>SO<sub>4</sub>/H<sub>3</sub>PO<sub>4</sub> (9:1, 360:40 mL) was added to a mixture of graphite plates (3.0 g) and KMnO<sub>4</sub> (18.0 g) and then stirred at 50 °C for 12 h. The reaction mixture was then poured onto a mixture of ice (400 mL) and H<sub>2</sub>O<sub>2</sub> (30%, 3 mL). The graphene oxide was washed and sequentially centrifuged with water, HCl (30%) and ethanol. The solid was filtered on a PTFE membrane (0.45 μm in diameter) and dried under vacuum at room temperature overnight. GO-Fe<sub>3</sub>O<sub>4</sub> was synthesized by the chemical combination of Fe<sup>2+</sup> and Fe<sup>3+</sup> in an alkaline solution in the presence of GO. GO (0.2 g) was suspended in 200 mL solution containing FeCl<sub>3</sub>·6H<sub>2</sub>O (2.34 g, 6.68 mmol) and FeCl<sub>2</sub>·4H<sub>2</sub>O (0.86 g, 4.33 mmol) at 50 °C in N<sub>2</sub> atmosphere. The solution was then sonicated for 10 min, and a solution of aqueous NH<sub>4</sub>OH (10 mL, 25%) was added dropwise to it under ultrasonic irradiation. The pH of the final mixture should be in the range of 10–11. To aid in the full growth of nanoparticle crystals, the reaction was uniformly stirred at 50 °C for 60 min. The precipitate was then separated by external magnetic field. The impurities in GO-Fe<sub>3</sub>O<sub>4</sub> were removed by washing with double distilled water, and the precipitate was separated by a permanent magnet. The GO-Fe<sub>3</sub>O<sub>4</sub> nanocomposite was then washed three times with 10 mL of ethanol and deionized water. Finally, the nanocomposite was dried under vacuum (Scheme 1).

### Preparation of polystyrene@graphene oxide-Fe<sub>3</sub>O<sub>4</sub> nanocomposite (PS@GO-Fe<sub>3</sub>O<sub>4</sub>)

For the production of PS@GO-Fe<sub>3</sub>O<sub>4</sub> nanocomposite, 0.3 g of GO-Fe<sub>3</sub>O<sub>4</sub> solution was dispersed in 20 mL of distilled water under ultrasound for 1 h. Then, the dispersed GO-Fe<sub>3</sub>O<sub>4</sub> solution was added to a solution of sodium dodecyl sulfate (SDS) surfactant (1.5 g) in distilled water (150 mL). The mixture was again sonicated for 30 min to prepare a homogeneous solution. Then, styrene monomer (4.5 g) was added and rapidly stirred. Afterward, 2,2'-azobis(2-methylpropionitrile) (AIBN, 0.15 g) was added to the solution for 30 min and stirred at 80 °C for 12 h in nitrogen atmosphere for polymerization. Finally, the PS@GO-Fe<sub>3</sub>O<sub>4</sub> nanocomposite was filtered and washed with methanol and deionized water several times and dried at 60 °C under vacuum for 24 h (Scheme 1) [51].



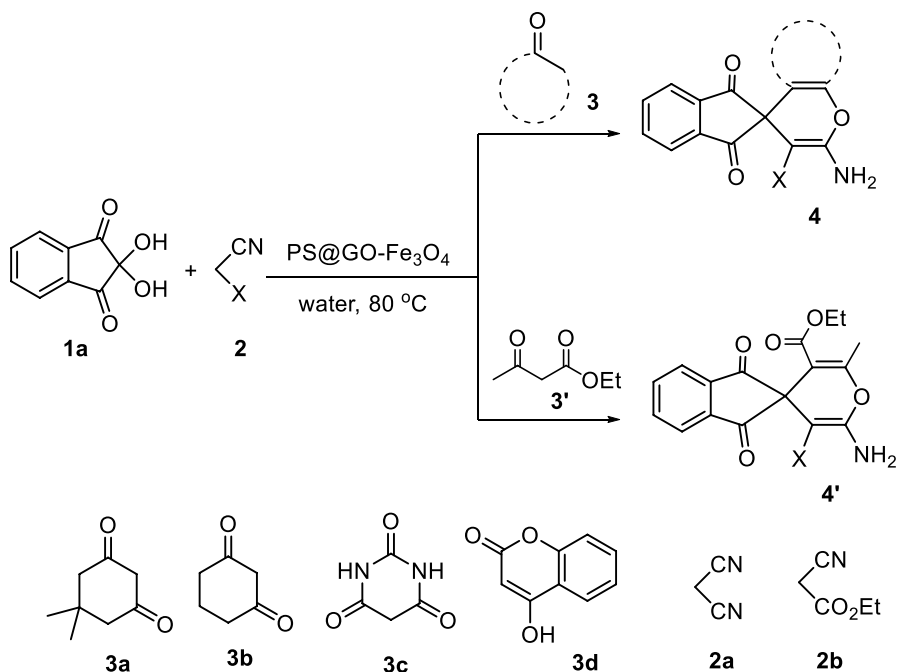
**Scheme 1** Schematic preparation route to PS@GO-Fe<sub>3</sub>O<sub>4</sub> nanocomposite

### General method for the three-component synthesis of 2'-aminospiro[indene-2, 4'-pyran]-3'-carbonitrile and 2'-aminospiro[indoline-3,4'-pyran]-3'-carbonitrile derivatives

In a round-bottomed flask, a mixture of ninhydrin/isatin (1 mmol), active methylene-containing compound (1 mmol) and PS@GO-Fe<sub>3</sub>O<sub>4</sub> (0.01 gr) in H<sub>2</sub>O (5 mL) was prepared and stirred at 80 °C for 5 min and then malononitrile (1 mmol) was added. After completion of the reaction as indicated by TLC (eluent, EtOAc: *n*-hexane, 1:2), the reaction mixture was left to cool to room temperature. Then, acetone (10 mL) was added to solve product and the catalyst was separated magnetically, washed with acetone and distilled water and dried at 60 °C under vacuum to reuse in the next cycle. The solvent of the reaction mixture was evaporated under vacuum to afford desired product. Further purification was performed by recrystallization in EtOH (Scheme 2, Table 2, entries 1–5).

### General procedure for the four-component synthesis of 2'-aminospiro[indeno[1,2-*b*]quinoxaline-11,4'-[4'H]pyran]-3-carbonitrile derivatives

A mixture of ninhydrin (1 mmol), *o*-phenylenediamine (1 mmol) and PS@GO-Fe<sub>3</sub>O<sub>4</sub> nanocomposite (0.01 gr) in ethanol (5 mL) was prepared and stirred at room temperature. After 10 min, malononitrile (1 mmol) and active methylene-containing compound (1 mmol) were added to the reaction mixture. The mixture was stirred for appropriate times according to Table 2 under reflux condition. Then, the reaction mixture was cooled to room temperature and acetone (10 mL) was added. The nano-magnetic catalyst was collected by an external magnet, washed several times with acetone and distilled water and dried at 60 °C under vacuum. The reaction solution was concentrated under vacuum, and the crude product was purified by recrystallization in EtOH (Scheme 3, Table 2, entries 6–14).



**Scheme 2** Three-component synthesis of 2'-aminospiro[indeno-2,4'-pyran]-3'-carbonitrile in the presence of PS@GO-Fe<sub>3</sub>O<sub>4</sub> nanocomposite

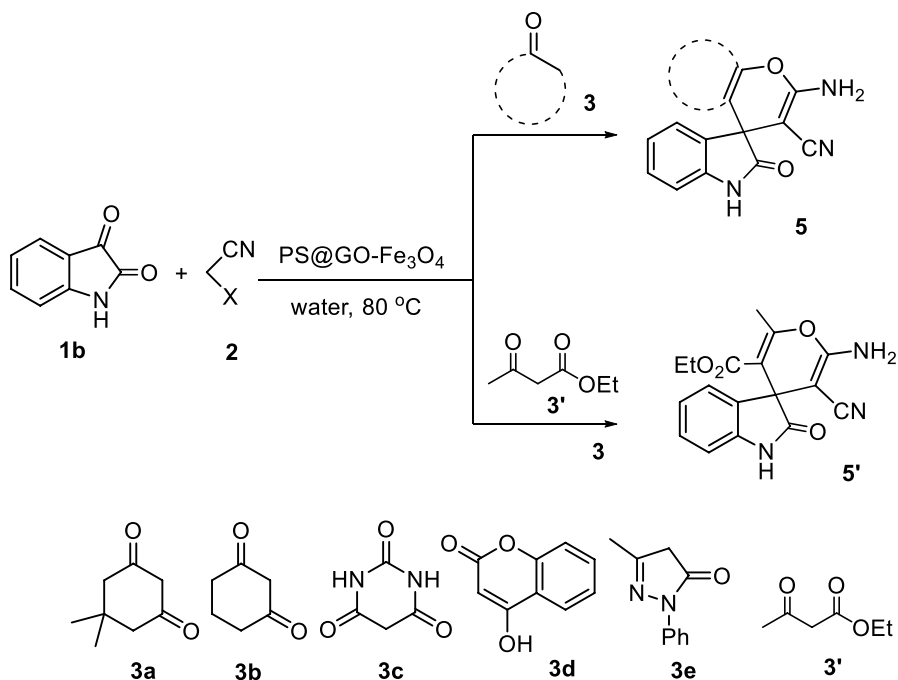
### Physical and spectral data of the products

2'-Amino-5',6',7',8'-tetrahydro-7',7'-dimethyl-1,3,5'-trioxospiro[indeno-2,4'-chromene]-3'-carbonitrile (**4a**), mp; 294–296 °C. FT-IR (KBr, cm<sup>-1</sup>): 3376, 3308, 3245, 3197, 2190, 1747, 1717, 1686, 1661, 1596. <sup>1</sup>H NMR (300 MHz, DMSO-d<sub>6</sub>, ppm): 1.03 (s, 6H, 2CH<sub>3</sub>), 2.19 (s, 2H, CH<sub>2</sub>), 2.67 (s, 2H, CH<sub>2</sub>), 7.64 (s, 2H, NH<sub>2</sub>), 7.99–8.05 (4H, ArH).

2'-Amino-5',6',7',8'-tetrahydro-1,3,5'-trioxospiro[indeno-2,4'-chromene]-3'-carbonitrile (**4b**), mp; 278–280 °C. FT-IR (KBr, cm<sup>-1</sup>): 3404, 3319, 3237, 3799, 2994, 2896, 2192, 1748, 1644, 1582. <sup>1</sup>H NMR (300 MHz, DMSO-d<sub>6</sub>, ppm): 1.95 (m, 2H, CH<sub>2</sub>), 2.27–2.30 (m, 2H, CH<sub>2</sub>), 2.70–2.73 (m, 2H, CH<sub>2</sub>), 7.63 (s, 2H, NH<sub>2</sub>), 2.99–8.05 (4H, ArH).

7'-Amino-1',2',3',4'-tetrahydro-1,2',3,4'-tetraoxospiro[indene-2,5'-[4'H]pyran[2,3-*d*]pyrimidine]-6'-carbonitrile (**4c**), mp; 190–192 °C. FT-IR (KBr, cm<sup>-1</sup>): 3425, 3301, 3278, 3215, 3138, 2198, 1722, 1705, 1642, 1623, 1520, 1334. <sup>1</sup>H NMR (300 MHz, DMSO-d<sub>6</sub>, ppm): 7.01 (s, 2H), 8.01(d, *J* = 8.5 Hz, 2H), 8.11 (d, *J* = 8.5 Hz, 2H), 9.08 (s, 1H), 11.03 (s, 1H).

2'-Amino-1,3,5'-trioxo-5'H-spiro[indene-2,4'-[4'H]pyrano[3,2-*c*]chromene]-3'-carbonitrile (**4d**), mp; 280 °C. FT-IR (KBr, cm<sup>-1</sup>): 3396, 3321, 3253, 3210, 2189, 1745, 1671, 1638, 1610, 1594. <sup>1</sup>H NMR (300 MHz, DMSO-d<sub>6</sub>, ppm): 7.51



**Scheme 3** Three-component synthesis of 2'-aminospiro[indoline-3,4'-pyran]-3'-carbonitrile in the presence of PS@GO-Fe<sub>3</sub>O<sub>4</sub> nanocomposite

(d,  $J=8.4$  Hz, 1H, ArH), 7.54 (t,  $J=7.65$  Hz, 1H, ArH), 7.78 (t,  $J=7.4$  Hz, 1H, ArH), 7.90 (d,  $J=7.75$  Hz, 1H, ArH), 8.09–8.13 (m, 4H, NH<sub>2</sub>, ArH).

Ethyl-2'-amino-3'-cyano-6'-methyl-1,3-dioxospiro[indeno-2,4'-[4'H]pyran]-5'-carboxylate (**4'**), mp; 224–226 °C. FT-IR (KBr, cm<sup>-1</sup>): 3338, 3183, 2934, 2190, 1675, 1637, 1429, 1278. <sup>1</sup>H NMR (300 MHz, DMSO-d<sub>6</sub>, ppm): 1.42 (m, 3H), 2.26 (s, 3H), 4.15–4.28 (m, 2H), 6.91 (s, 2H, NH<sub>2</sub>), 7.81–7.76 (m, 1H, ArH), 7.99–7.84 (m, 3H, ArH).

Ethyl-7'-amino-1',2',3',4'-tetrahydro-1,2',3,4'-tetraoxospiro[indene-2,5'-[4'H]pyrano[2,3-*d*]pyrimidine]-6'-carboxylate (**4e**), mp; 223–225 °C. FT-IR (KBr, cm<sup>-1</sup>): 3428, 3305, 3266, 3215, 3141, 2197, 1720, 1697, 1639, 1623, 1518, 1329. <sup>1</sup>H NMR (300 MHz, DMSO-d<sub>6</sub>, ppm): 1.06 (t,  $J=7.6$  Hz, 3H), 3.95 (q,  $J=7.6$  Hz, 2H), 8.03 (d,  $J=8.7$  Hz, 2H), 8.06 (d,  $J=8.7$  Hz, 2H), 9.11 (s, 1H), 10.96 (s, 1H).

2'-Amino-5',6',7',8'-tetrahydro-7',7'-dimethyl-2,5'-dioxospiro[indoline-3,4'-chromene]-3'-carbonitrile (**5a**), mp; 292–294 °C. FT-IR (KBr, cm<sup>-1</sup>): 3376, 3312, 3144, 2928, 2196, 1724, 1656, 1348, 1224, 1056. <sup>1</sup>H NMR (300 MHz, DMSO-d<sub>6</sub>, ppm): 1.00 (s, 3H), 1.03 (s, 3H), 2.08–2.19 (m, 2H), 2.56 (s, 2H), 6.78 (d,  $J=7.3$  Hz, 1H, ArH), 6.89 (t,  $J=7.3$  Hz, 1H, ArH), 6.97 (d,  $J=7.3$  Hz, 1H, ArH), 7.14 (t,  $J=7.3$  Hz, 1H, ArH), 7.23 (s, 2H, NH<sub>2</sub>), 10.40 (s, 1H, NH).

2'-Amino-5',6',7',8'-tetrahydro-2,5'-dioxospiro[indoline-3,4'-chromene]-3'-carbonitrile (**5b**), mp; 297–299 °C. FT-IR (KBr, cm<sup>-1</sup>): 3352, 3296, 3176, 2952, 2204, 1712, 1656, 1352, 1216, 1076. <sup>1</sup>H NMR (300 MHz, DMSO-d<sub>6</sub>, ppm):

1.91–2.00 (m, 2H), 2.10–2.30 (m, 2H), 2.62–2.73 (m, 2H), 6.78 (d,  $J=7.4$  Hz, 1H, ArH), 6.88 (t,  $J=7.4$  Hz, 1H, ArH), 7.00 (d,  $J=7.4$  Hz, 1H, ArH), 7.16 (t,  $J=7.4$  Hz, 1H, ArH), 7.23 (s, 2H, NH<sub>2</sub>), 10.40 (s, 1H, NH).

7'-amino-1',2',3',4'-tetrahydro-2,2',4'-trioxospiro[indoline-3,5'-[4'H]pyrano[2,3-*d*]pyrimidine]-6'-carbonitrile (**5c**), mp; 296–298 °C. FT-IR (KBr, cm<sup>-1</sup>): 3559, 3286, 3215, 3199, 1717, 1642, 1324. <sup>1</sup>H NMR (300 MHz, DMSO-d<sub>6</sub>, ppm): 6.95 (s, 2H), 7.05 (t,  $J=8.3$  Hz, 1H), 7.21–7.30 (m, 3H), 9.03 (s, 1H), 9.66 (s, 1H), 11.03 (s, 1H).

2'-amino-2,5'-dioxospiro[indoline-3,4'-[4'H]pyrano[3,2-*c*]chromene]-3'-carbonitrile (**5d**), mp; 286–289 °C. FT-IR (KBr, cm<sup>-1</sup>): 3397, 3296, 3196, 2206, 1710, 1674, 1604, 1359. <sup>1</sup>H NMR (300 MHz, DMSO-d<sub>6</sub>, ppm): 6.84–6.93 (m, 2H, ArH), 7.16–7.23 (m, 2H, ArH), 7.49–7.58 (m, 2H, ArH), 7.69 (s, 2H, NH<sub>2</sub>), 7.75–7.80 (t,  $J=7.38$  Hz, 1H, ArH), 7.93 (d,  $J=7.92$  Hz, 1H, ArH), 10.70 (s, 1H, NH).

6'-amino-3'-methyl-2-oxo-1'-phenylspiro[indoline-3,4'-pyrano[2,3-*c*]pyrazole]-5'-carbonitrile (**5e**), mp; 250–252 °C. FT-IR (KBr, cm<sup>-1</sup>): 3411, 3330, 3270, 2193, 1716, 1625, 1323. <sup>1</sup>H NMR (300 MHz, DMSO-d<sub>6</sub>, ppm): 1.54 (s, 3H), 6.94 (d,  $J=7.7$  Hz, 1H, ArH), 7.03 (t,  $J=7.4$  Hz, 1H, ArH), 7.18 (d,  $J=7.3$  Hz, 1H, ArH), 7.28 (t,  $J=7.6$  Hz, 1H, ArH), 7.35 (t,  $J=7.9$  Hz, 1H, ArH), 7.52 (t,  $J=7.9$  Hz, 2H, ArH), 7.57 (s, 2H, NH<sub>2</sub>), 7.78 (d,  $J=7.9$  Hz, 2H, ArH), 10.74 (s, 1H, NH).

Ethyl-2'-amino-3'-cyano-6'-methyl-2-oxospiro[indoline-3,4'-[4'H]pyran]-5'-carboxylate (**5'**), mp; 268–270 °C. FT-IR (KBr, cm<sup>-1</sup>): 3480, 3275, 3158, 2976, 2188, 1723, 1710, 1676, 1618. <sup>1</sup>H NMR (300 MHz, DMSO-d<sub>6</sub>, ppm): 0.74 (t,  $J=7.0$  Hz, 3H), 2.29 (s, 3H), 3.71–3.82 (m, 2H), 6.75 (d,  $J=7.6$  Hz, 1H, ArH), 6.90 (t,  $J=7.3$  Hz, 1H, ArH), 7.00 (d,  $J=7.1$  Hz, 1H, ArH), 7.16 (s, 2H, NH<sub>2</sub>), 7.18 (t,  $J=7.6$  Hz, 1H, ArH), 10.41 (s, 1H, NH).

2'-amino-5',6',7',8'-tetrahydro-7',7'-dimethyl-5-oxospiro[indeno[1,2-*b*]quinoxaline-11,4'-[4'H]pyran]-3'-carbonitrile (**7a**), mp; 280–282 °C. FT-IR (KBr, cm<sup>-1</sup>): 3460, 3300, 3170, 2960, 2196, 1600, 1352. <sup>1</sup>H NMR (300 MHz, DMSO-d<sub>6</sub>, ppm): 1.00 (s, 3H, CH<sub>3</sub>), 1.03 (s, 3H, CH<sub>3</sub>), 1.97–2.08 (m, 2H, CH<sub>2</sub>), 2.61–2.75 (m, 2H, CH<sub>2</sub>), 7.33 (s, 2H, NH<sub>2</sub>), 7.51–7.55 (m, 2H, ArH), 7.59–7.60 (m, 1H, ArH), 7.75–7.78 (m, 1H, ArH), 7.81–7.84 (m, 1H, ArH), 8.05 (dd,  $J=1.5$ , 8.2 Hz, 1H, ArH), 8.08 (d,  $J=7.5$  Hz, 1H, ArH), 8.15 (dd,  $J=1.0$ , 8.0 Hz, 1H, ArH).

2'-amino-5',6',7',8'-tetrahydro-5'-oxospiro[indeno[1,2-*b*]quinoxaline-11,4'-[4'H]pyran]-3'-carbonitrile (**7b**), mp; 275–277 °C. FT-IR (KBr, cm<sup>-1</sup>): 3360, 3280, 3165, 2920, 2194, 1670, 1600, 1330. <sup>1</sup>H NMR (300 MHz, DMSO-d<sub>6</sub>, ppm): 1.89–1.94 (m, 2H, CH<sub>2</sub>), 2.07–2.14 (m, 2H, CH<sub>2</sub>), 2.73–2.81 (m, 2H, CH<sub>2</sub>), 7.33 (s, 2H, NH<sub>2</sub>), 7.52–7.61 (m, 2H, ArH), 7.75–7.84 (m, 2H, ArH), 8.06–8.09 (m, 2H, ArH), 8.16 (dd,  $J=1.0$ , 8.0 Hz, 1H, ArH).

6'-amino-3'-methyl-1'-phenylspiro[indeno[1,2-*b*]quinoxaline-11,4'-[1'H]pyrano[2,3-*c*]pyrazole]-5'-carbonitrile (**7c**), mp; 240–242 °C. FT-IR (KBr, cm<sup>-1</sup>): 3321, 3292, 3145, 2920, 2204, 1653, 1591, 1517, 1392. <sup>1</sup>H NMR (300 MHz, DMSO-d<sub>6</sub>, ppm): 1.10 (s, 3H, CH<sub>3</sub>), 7.37 (t,  $J=7.5$  MHz, 1H, ArH), 7.54 (t,  $J=7.7$  MHz, 2H, ArH), 7.64–7.71 (m, 5H, ArH), 7.81–7.90 (m, 4H, ArH), 8.12 (d,  $J=8.5$  MHz, 1H, ArH), 8.20 (t,  $J=8.5$  MHz, 2H).

2'-amino-5',6',7',8'-tetrahydro-4,7',7'-trimethyl-5-oxospiro[indeno[1,2-*b*]quinoxaline-11,4'-[4H]pyran]-3'-carbonitrile (**7d**), mp; 274–276 °C. FT-IR (KBr,  $\text{cm}^{-1}$ ): 3444, 3313, 3047, 2954, 2192, 1666, 1595, 1350.  $^1\text{H}$  NMR (300 MHz,  $\text{DMSO-d}_6$ , ppm): 1.03 (s, 3H,  $\text{CH}_3$ ), 1.05 (s, 3H,  $\text{CH}_3$ ), 1.97–2.07 (dd,  $J=16.2$ , 19.5 Hz, 2H,  $\text{CH}_2$ ), 2.59 (s, 3H,  $\text{CH}_3$ ), 2.67–2.79 (dd,  $J=17.7$ , 26.1 Hz, 2H,  $\text{CH}_2$ ), 7.33 (s, 2H,  $\text{NH}_2$ ), 7.51–7.61 (m, 3H, ArH), 7.93 (s, 1H, ArH), 7.97 (d,  $J=2.4$  Hz, 2H, ArH), 8.09 (d,  $J=3.4$  Hz, 1H, ArH).  $^{13}\text{C}$  NMR (75 MHz,  $\text{DMSO-d}_6$ , ppm): 21.3, 27.1, 29.2, 32.8, 34.6, 51.0, 51.8, 75.3, 108.6, 114.5, 121.9, 125.8, 126.8, 128.3, 128.4, 128.6, 131.9, 134.3, 136.9, 138.1, 141.8, 142.1, 151.5, 158.0, 166.1, 168.5, 194.2. HRMS (EI) Found:  $\text{M}^+$ , 434.1744.  $\text{C}_{27}\text{H}_{22}\text{N}_4\text{O}_2$ : requires  $\text{M}^+$ , 434.1743. Anal. Calcd. for  $\text{C}_{27}\text{H}_{22}\text{N}_4\text{O}_2$ : C 74.65, H 5.07, N 12.90; found C 74.57, H 5.11, N 12.88%.

2'-amino-5',6',7',8'-tetrahydro-4-methyl-5'-oxospiro[indeno[1,2-*b*]quinoxaline-11,4'-[4H]pyran]-3'-carbonitrile (**7e**); mp; 266–268 °C. FT-IR (KBr,  $\text{cm}^{-1}$ ): 3352, 3284, 3242, 2920, 2198, 1672, 1598, 1350.  $^1\text{H}$  NMR (300 MHz,  $\text{DMSO-d}_6$ , ppm): 1.89–1.94 (m, 2H,  $\text{CH}_2$ ), 2.03 (m, 2H,  $\text{CH}_2$ ), 2.59 (s, 3H,  $\text{CH}_3$ ), 2.79 (m, 2H,  $\text{CH}_2$ ), 7.37 (s, 2H,  $\text{NH}_2$ ), 7.50–7.61 (m, 3H, ArH), 7.93 (s, 1H, ArH), 7.97 (d,  $J=2.4$  Hz, 2H, ArH), 8.07 (d,  $J=6.6$  Hz, 1H, ArH).  $^{13}\text{C}$  NMR (75 MHz,  $\text{DMSO-d}_6$ , ppm): 21.1, 21.5, 28.3, 37.0, 48.1, 58.3, 113.6, 118.3, 122.7, 126.2, 128.3, 128.6, 129.1, 129.5, 131.2, 139.1, 142.2, 142.3, 145.1, 152.7, 158.4, 160.6, 164.9, 166.1, 194.9. HRMS (EI) Found:  $\text{M}^+$ , 406.1431.  $\text{C}_{25}\text{H}_{18}\text{N}_4\text{O}_2$ : requires  $\text{M}^+$ , 406.1430. Anal. Calcd. for  $\text{C}_{25}\text{H}_{18}\text{N}_4\text{O}_2$ : C 73.89, H 4.43, N 13.79; found C 73.94, H 4.51, N 13.72%.

6'-amino-3',4-dimethyl-1'-phenylspiro[indeno[1,2-*b*]quinoxaline-11,4'-[1H]pyrano[2,3-*c*]pyrazole]-5'-carbonitrile (**7f**), mp; 207–210 °C. FT-IR (KBr,  $\text{cm}^{-1}$ ): 3311, 3290, 3139, 2914, 2200, 1652, 1591, 1519, 1392.  $^1\text{H}$  NMR (300 MHz,  $\text{DMSO-d}_6$ , ppm): 1.09 (s, 3H), 2.47 (s, 3H), 7.36 (s, 2H,  $\text{NH}_2$ ), 7.51 (d,  $J=7.5$  MHz, 2H), 7.63–7.64 (m, 5H), 7.81–7.90 (m, 4H), 8.16 (s, 1H).

2'-amino-5',6',7',8'-tetrahydro-3,4,7',7'-tetramethyl-5-oxospiro[indeno[1,2-*b*]quinoxaline-11,4'-[4H]pyran]-3'-carbonitrile (**7g**), mp; 222–224 °C. FT-IR (KBr,  $\text{cm}^{-1}$ ): 3436, 3334, 3155, 2950, 2192, 1675, 1600, 1348.  $^1\text{H}$  NMR (300 MHz,  $\text{DMSO-d}_6$ , ppm): 1.028 (s, 3H,  $\text{CH}_3$ ), 1.047 (s, 3H,  $\text{CH}_3$ ), 1.97–2.10 (dd,  $J=16.2$ , 20.4 Hz, 2H,  $\text{CH}_2$ ), 2.46 (s, 3H,  $\text{CH}_3$ ), 2.50 (s, 3H,  $\text{CH}_3$ ), 2.62–2.77 (dd,  $J=16.8$ , 26.1 Hz, 2H,  $\text{CH}_2$ ), 7.34 (s, 2H,  $\text{NH}_2$ ), 7.51–7.61 (m, 3H, ArH), 7.82 (s, 1H, ArH), 7.95 (s, 1H, ArH), 8.07 (d,  $J=7.2$  MHz, 1H, ArH).  $^{13}\text{C}$  NMR (75 MHz,  $\text{DMSO-d}_6$ , ppm): 18.8, 18.9, 27.4, 28.3, 32.3, 35.1, 50.8, 51.7, 76.4, 109.0, 114.7, 121.6, 125.6, 126.4, 128.4, 128.6, 128.7, 131.9, 137.7, 139.2, 141.1, 147.3, 148.2, 151.6, 157.0, 165.8, 167.1, 168.2, 194.5. HRMS (EI) Found:  $\text{M}^+$ , 448.1897.  $\text{C}_{28}\text{H}_{24}\text{N}_4\text{O}_2$ : requires  $\text{M}^+$ , 448.1899. Anal. Calcd. for  $\text{C}_{28}\text{H}_{24}\text{N}_4\text{O}_2$ : C 75.00, H 5.36, N 12.50; found C 74.93, H 5.42, N 12.47%.

2'-amino-5',6',7',8'-tetrahydro-3,4-dimethyl-5-oxospiro[indeno[1,2-*b*]quinoxaline-11,4'-[4H]pyran]-3'-carbonitrile (**7h**), mp; 275–277 °C. FT-IR (KBr,  $\text{cm}^{-1}$ ): 3394, 3352, 3278, 2918, 2192, 1675, 1600, 1338.  $^1\text{H}$  NMR (300 MHz,  $\text{DMSO-d}_6$ , ppm): 1.89–1.94 (m, 2H,  $\text{CH}_2$ ), 2.03 (m, 2H,  $\text{CH}_2$ ), 2.47 (s, 3H,  $\text{CH}_3$ ), 2.59 (s, 3H,  $\text{CH}_3$ ), 2.80 (m, 2H,  $\text{CH}_2$ ), 7.37 (s, 2H,  $\text{NH}_2$ ), 7.51–7.61 (m, 3H, ArH), 7.93 (s, 1H, ArH), 7.97 (s, 1H, ArH), 8.07 (d,  $J=7.2$  Hz, 1H, ArH).  $^{13}\text{C}$  NMR

(75 MHz, DMSO-d<sub>6</sub>, ppm): 18.6, 18.7, 20.5, 27.7, 37.3, 48.2, 58.3, 111.5, 118.4, 121.7, 125.3, 128.6, 128.8, 129.5, 129.6, 129.7, 141.6, 142.3, 147.9, 154.7, 155.2, 157.8, 158.4, 164.4, 194.6. HRMS (EI) Found: M<sup>+</sup>, 420.1588. C<sub>26</sub>H<sub>20</sub>N<sub>4</sub>O<sub>2</sub>: requires M<sup>+</sup>, 420.1586. Anal. Calcd. for C<sub>26</sub>H<sub>20</sub>N<sub>4</sub>O<sub>2</sub>: C 74.29, H 4.76, N 13.33; found C 74.32, H 4.71, N 13.35%.

6'-amino-3,4,3'-trimethyl-1'-phenylspiro[indeno[1,2-*b*]quinoxaline-11,4'-[1'H]pyrano[2,3-*c*]pyrazole]-5'-carbonitrile (**7i**), mp; 248–250 °C). FT-IR (KBr, cm<sup>-1</sup>): 3336, 3296, 3155, 2916, 2200, 1652, 1595, 1521, 1394. <sup>1</sup>H NMR (300 MHz, DMSO-d<sub>6</sub>, ppm): 1.09 (s, 3H, CH<sub>3</sub>), 2.42 (s, 3H, CH<sub>3</sub>), 2.47 (s, 3H, CH<sub>3</sub>), 7.36 (t, *J*=7.2 Hz, 1H, ArH), 7.51 (t, *J*=7.7 Hz, 2H, ArH), 7.63–7.64 (m, 5H, ArH), 7.85 (d, *J*=9.0 Hz, 3H, ArH), 7.97 (s, 1H, ArH), 8.14 (t, *J*=3.7 Hz, 1H, ArH).

## Results and discussion

### Characterizations of nanocomposite

At first, the polystyrene-coated magnetic graphene oxide (PS@GO-Fe<sub>3</sub>O<sub>4</sub>) was prepared by a two-step procedure as explained in Experimental section. Then, this magnetic nanocomposite was characterized by Fourier infrared spectroscopy (FT-IR), scanning electron microscopy (SEM) and vibrating sample magnetometry (VSM) analyses. The FT-IR spectra of GO, GO-Fe<sub>3</sub>O<sub>4</sub>, polystyrene and PS@GO-Fe<sub>3</sub>O<sub>4</sub> nanocomposite are shown in Fig. 1. In Fig. 1a, a broad absorption band in

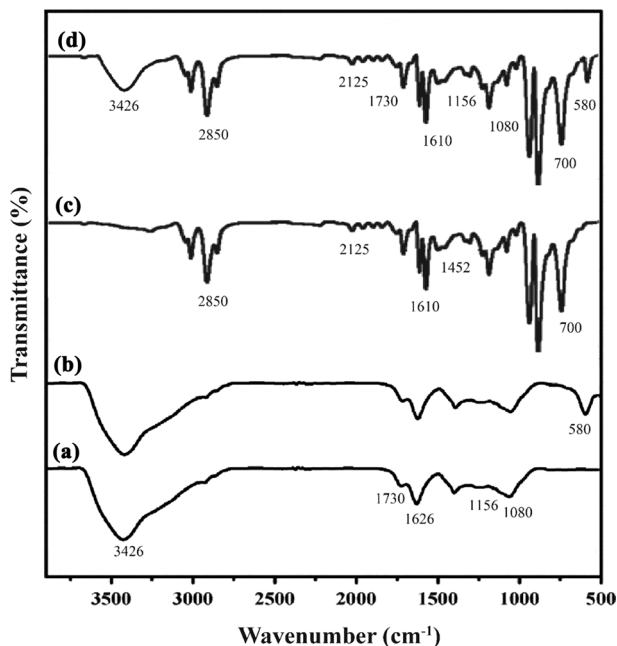


Fig. 1 FT-IR spectra of (a) GO, (b) GO-Fe<sub>3</sub>O<sub>4</sub>, (c) polystyrene and (d) PS@GO-Fe<sub>3</sub>O<sub>4</sub>

3426  $\text{cm}^{-1}$  is related to the stretching vibration of O–H and shows the presence of oxygen-containing functional groups in graphene oxide. The stretching vibrations of C=O, aromatic C=C and epoxy and alkoxy C–O groups are observed in 1730, 1626, 1156 and 1080, respectively. In the FT-IR spectrum of GO-Fe<sub>3</sub>O<sub>4</sub> nanocomposite (Fig. 1b), an absorption band is present at 580  $\text{cm}^{-1}$  that belongs to the Fe–O vibration. In the FT-IR spectrum of polystyrene (Fig. 1c), the stretching vibration of CH, the bending vibration of CH<sub>2</sub>, the stretching vibration of C=C, the bending vibration of C–C and the out-of-plane bending vibration of C–H are seen at 2125, 2850, 1610, 1452 and 700  $\text{cm}^{-1}$ , respectively [51]. In FT-IR spectrum of PS@GO-Fe<sub>3</sub>O<sub>4</sub> nanocomposite (Fig. 1d), all characteristic peaks of GO-Fe<sub>3</sub>O<sub>4</sub> (1b) and polystyrene (1c) spectra are observable. This spectrum (1d) indicates that the surface of GO-Fe<sub>3</sub>O<sub>4</sub> is well covered by polystyrene [51].

The TEM graph of graphene oxide (Fig. 2) shows a flake-like sheet structure. The TEM image of PS@GO-Fe<sub>3</sub>O<sub>4</sub> nanocomposite exhibits the uniform distribution of iron oxide nanoparticles on the surface of GO nanosheets. Furthermore, the different morphology appearance of nanocomposite compared to graphene oxide confirms that Fe<sub>3</sub>O<sub>4</sub> nanoparticles have been satisfactorily formed on the GO-Fe<sub>3</sub>O<sub>4</sub> surface.

As the VSM analyses of GO and PS@GO-Fe<sub>3</sub>O<sub>4</sub> (Fig. 3) nanocomposite show, the magnetic remanences in both graphs are close to zero. This means that by removing the external magnetic field, the magnetic property disappears. Therefore, both GO-Fe<sub>3</sub>O<sub>4</sub> and PS@GO-Fe<sub>3</sub>O<sub>4</sub> show superparamagnetic behavior. Reducing the SM value of PS@GO-Fe<sub>3</sub>O<sub>4</sub> nanocomposite relative to GO-Fe<sub>3</sub>O<sub>4</sub> is due to the fact that the GO-Fe<sub>3</sub>O<sub>4</sub> surface is coated with a layer of polystyrene and confirms the successful formation of PS@GO-Fe<sub>3</sub>O<sub>4</sub> nanocomposite [51].

After characterization of PS@GO-Fe<sub>3</sub>O<sub>4</sub> nanocomposite, its catalytic activity was studied in the three-component synthesis of 2-aminospiro[chromene-4,2'-indene]-3-carbonitrile. Initially, the reaction of ninhydrin **1a**, malononitrile **2a** and dimedone **3a** in water was selected as model reaction (Scheme 2). Different catalysts including 1,3-dibromo-5,5-dimethylhydantoin (DBH), trichloroicyanuric acid (TCA), Bi(NO<sub>3</sub>)<sub>3</sub>·5H<sub>2</sub>O, ZrCl<sub>4</sub> and tungstophosphoric acid (TPA) have been used in the

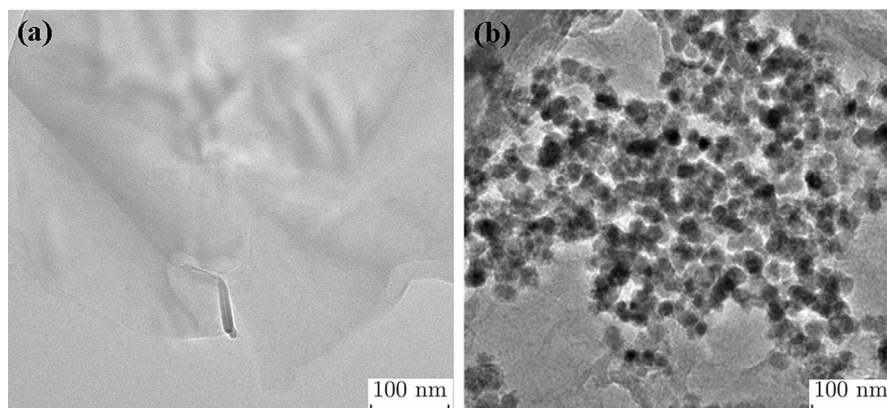


**Fig. 2** TEM graph of **a** graphene oxide and **b** PS@GO-Fe<sub>3</sub>O<sub>4</sub>

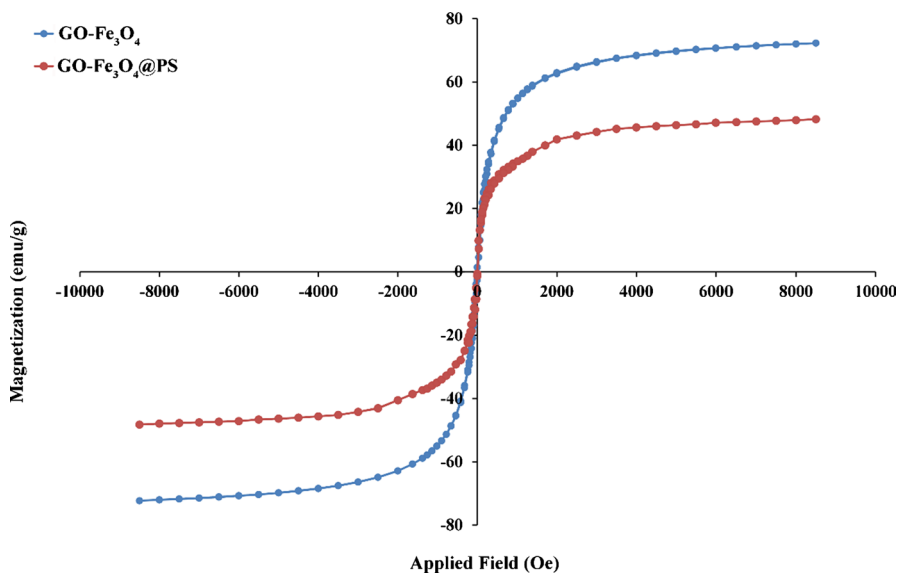


**Fig. 3** VSM curves of GO-Fe<sub>3</sub>O<sub>4</sub> and PS@GO-Fe<sub>3</sub>O<sub>4</sub> nanocomposites

model reaction (Table 1, entries 1–5). As shown in Table 1, all of these reactions were performed for long times and poor yields of products were obtained. Then, the catalytic activity of PS@GO-Fe<sub>3</sub>O<sub>4</sub> nanocomposite was examined in the model reaction which led to an acceptable yield in short time (Table 1, entry 6).

So, the reaction conditions were optimized in the presence of PS@GO-Fe<sub>3</sub>O<sub>4</sub> nanocomposite. To this aim, different amounts of catalyst, various solvents and different temperatures were examined in the model reaction (Table 1, entry 6–15). The best result was obtained in the reaction of ninhydrin **1a** (1 mmol), malononitrile **2a** (1 mmol) and dimedone **3a** (1 mmol) in the presence of nanocatalyst (10 mg) in water (5 ml) at 80 °C (Table 1, entry 7). Corresponding 2'-amino-5',6',7',8'-tetrahydro-7',7'-dimethyl-1,3,5'-trioxospiro[indeno-2,4'-chromene]-3'-carbonitrile **4a** was generated in 93% yield after 2 h.

The model reaction was also performed in the presence of PS, GO and Fe<sub>3</sub>O<sub>4</sub> nanoparticles that low catalytic activities were observed for them (Table 1, entry 16–18). Furthermore, the model reaction was down in the absence of catalyst to show the efficiency of the nanomagnetic catalyst. Analysis of the reaction mixture showed that no product was found even after 8 h (Table 1, entry 19).

To scope the generality of this method, the three-component condensations of ninhydrin **1a**, malononitrile **2a**/ethyl cyanoacetate **2b** and compounds containing active methylene group **3** (dimedone **3a**, 1,3-cyclohexanedione **3b**, barbituric acid **3c**, 4-hydroxycoumarin **3d** and ethyl acetoacetate **3'**) were performed in the presence of PS@GO-Fe<sub>3</sub>O<sub>4</sub> nanocomposite under optimized reaction conditions (Scheme 2, Table 2, entries 1–6). As shown in Table 2, corresponding 2-aminospiro[indeno-2,4'-pyran]-3'-carbonitriles **4** & **4'** were generated in high yields. In the next step, the catalytic activity of PS@GO-Fe<sub>3</sub>O<sub>4</sub> was studied in the

**Table 1** Application of various catalysts and optimization of the conditions in the reaction of ninhydrin **1**, malononitrile **2a** and dimedone **3a**

Entry <sup>a</sup>	Catalyst (mg)	Solvent	Temp (°C)	Time (h)	Yield <sup>b</sup> (%)
1	DBDMH (10)	H <sub>2</sub> O	100	5	30
2	TCA (10)	H <sub>2</sub> O	100	3	Trace
3	Bi(NO <sub>3</sub> ) <sub>3</sub> ·5H <sub>2</sub> O (10)	H <sub>2</sub> O	100	5	40
4	ZrCl <sub>4</sub> (10)	H <sub>2</sub> O	100	4	30
5	TPA (10)	H <sub>2</sub> O	100	4	20
6	PS@GO-Fe <sub>3</sub> O <sub>4</sub> (10)	H <sub>2</sub> O	100	2	90
7	PS@GO-Fe <sub>3</sub> O <sub>4</sub> (10)	H <sub>2</sub> O	80	2	93
8	PS@GO-Fe <sub>3</sub> O <sub>4</sub> (10)	H <sub>2</sub> O	50	2	65
9	PS@GO-Fe <sub>3</sub> O <sub>4</sub> (5)	H <sub>2</sub> O	80	2	70
10	PS@GO-Fe <sub>3</sub> O <sub>4</sub> (15)	H <sub>2</sub> O	80	2	90
11	PS@GO-Fe <sub>3</sub> O <sub>4</sub> (10)	EtOH	80	3	70
12	PS@GO-Fe <sub>3</sub> O <sub>4</sub> (10)	EtOH:H <sub>2</sub> O (1:1)	80	3	40
13	PS@GO-Fe <sub>3</sub> O <sub>4</sub> (10)	CH <sub>3</sub> CN	80	3	30
14	PS@GO-Fe <sub>3</sub> O <sub>4</sub> (10)	MeOH	80	3	65
15	PS@GO-Fe <sub>3</sub> O <sub>4</sub> (10)	Acetone	80	3	Trace
16	Fe <sub>3</sub> O <sub>4</sub> (10)	H <sub>2</sub> O	80	3	50
17	GO (10)	H <sub>2</sub> O	80	3	30
18	PS (10)	H <sub>2</sub> O	80	3	15
19	–	H <sub>2</sub> O	80	8	10

<sup>a</sup>1 mmol of all starting materials was used

<sup>b</sup>Isolated yields

reaction of isatin **1b** with malononitrile **2a** and active methylene-containing compounds **3** such as dimedone, 1,3-cyclohexanedione, barbituric acid, 4-hydroxy coumarin, 1-phenyl-3-methylpyrazoline-5-one and ethyl acetoacetate **3'** under optimized reaction conditions (Scheme 3). Fortunately, desired products **5 & 5'** were generated in high-to-excellent yields (Table 2, entries 7–12).

Then, we examined the catalytic activity of PS@GO-Fe<sub>3</sub>O<sub>4</sub> in the one-pot four-component synthesis of 2'-aminospiro[indeno[1,2-*b*]quinoxaline-11,4'-pyran]-3'-carbonitrile. To this aim, equimolar amounts of ninhydrin **1a**, o-phenylenediamine **6a**, malononitrile **2a** and dimedone **3a** reacted in the presence of PS@GO-Fe<sub>3</sub>O<sub>4</sub> in water and the desired product was obtained in 10% yield after 2 h under optimized condition (Scheme 4). To improve the result, different solvents and temperatures were applied in this reaction. Finally, ethanol was chosen as the best solvent under reflux condition and corresponding 2'-amino-5',6',7',8'-tetrahydro-7',7'-dimethyl-5-oxospiro[indeno[1,2-*b*]quinoxaline-11,4'-[4'<sup>H</sup>]pyran]-3'-carbonitrile **7a** was obtained in 87% yield after 2.5 h (Table 2, entry 13). Similarly, the reactions of ninhydrin **1a**, various o-phenylenediamines **6**, malononitrile **2a** and different active methylene-containing compounds **3** were performed in ethanol under reflux condition to afford expected products as the

**Table 2** Syntheses of indene derivatives catalyzed by nanomagnetic PS@GO-Fe<sub>3</sub>O<sub>4</sub>

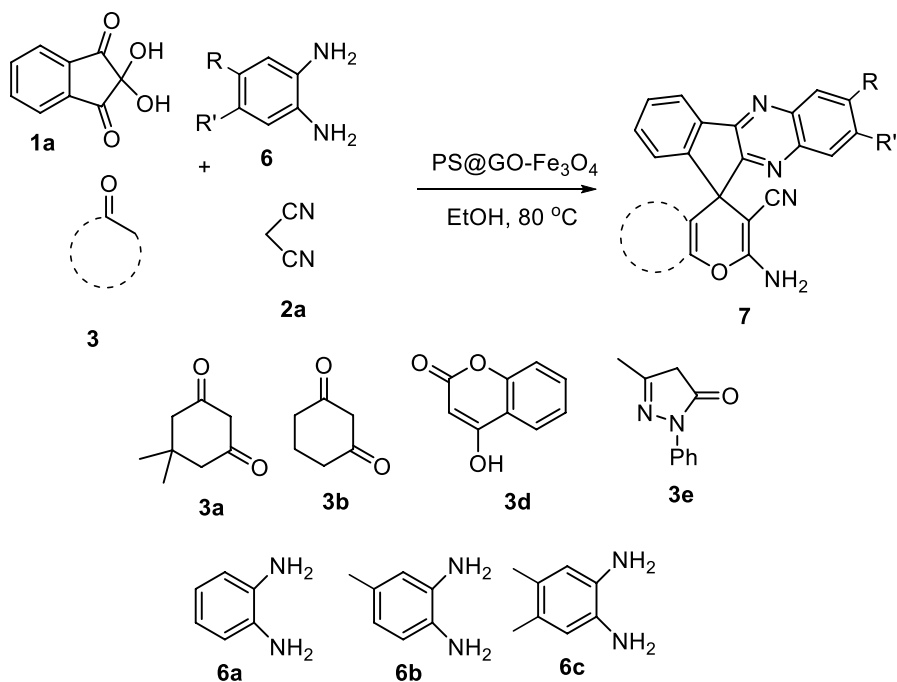
Entry	1	2	3	6	Product	Time (h)	Yield (%) <sup>a</sup>	Mp (°C) [Ref.]
1	1a	2a	3a	–	4a	2	93	290–292 [51]
2	1a	2a	3b	–	4b	2	85	274–280 [51]
3	1a	2a	3c	–	4c	1	87	190–192 [52]
4	1a	2a	3d	–	4d	3	90	280 [51]
5	1a	2a	3'	–	4'	5.5	73	224–226 [53]
6	1a	2b	3c	–	4e	2	95	223–225 [52]
7	1b	2a	3a	–	5a	0.5	96	292–294 [52]
8	1b	2a	3b	–	5b	0.4	90	297–299 [52]
9	1b	2a	3c	–	5c	0.8	95	296–298 [52]
10	1b	2a	3d	–	5d	0.8	95	286–289 [52]
11	1b	2a	3e	–	5e	1.5	80	250–252 [52]
12	1b	2a	3'	–	5'	3	80	268–270 [53]
13	1a	2a	3a	6a	7a	2.5	87	280–282 [25]
14	1a	2a	3b	6a	7b	4	73	275–277 [25]
15	1a	2a	3e	6a	7c	4	65	240–242 [25]
16	1a	2a	3a	6b	7d	3	95	274–276
17	1a	2a	3b	6b	7e	1.5	75	266–268
18	1a	2a	3e	6b	7f	1.5	97	207–210 [54]
19	1a	2a	3a	6c	7g	4	90	222–224
20	1a	2a	3b	6c	7h	4	68	275–277
21	1a	2a	3e	6c	7i	2.5	82	248–250 [25]

<sup>a</sup>Isolated yields

times and yields reported in Table 2 (entries 13–21). So, the present magnetic nanocatalyst can be efficiently used for the three- and four-component synthesis of spiro indene and spiro indoline derivatives.

Although the actual mechanism for the synthesis of 2'-aminospiro[indeno-2,4'-pyran]-3'-carbonitrile catalyzed by PS@GO-Fe<sub>3</sub>O<sub>4</sub> is unclear, a plausible mechanism has been proposed in Scheme 5.

In the next step, the reusability of PS@GO-Fe<sub>3</sub>O<sub>4</sub> nanocatalyst was investigated in the reaction of ninhydrin, dimedone and malononitrile in optimized reaction conditions. After completion of the reaction, the catalyst was separated by an external magnet, washed with acetone and dried under vacuum at 60 °C for 2 h. The recovered catalyst was then reused in the same reaction. The recovery and reuse of PS@GO-Fe<sub>3</sub>O<sub>4</sub> were performed eight times (Table 3), and its catalytic activity did not reduce significantly after eight runs.

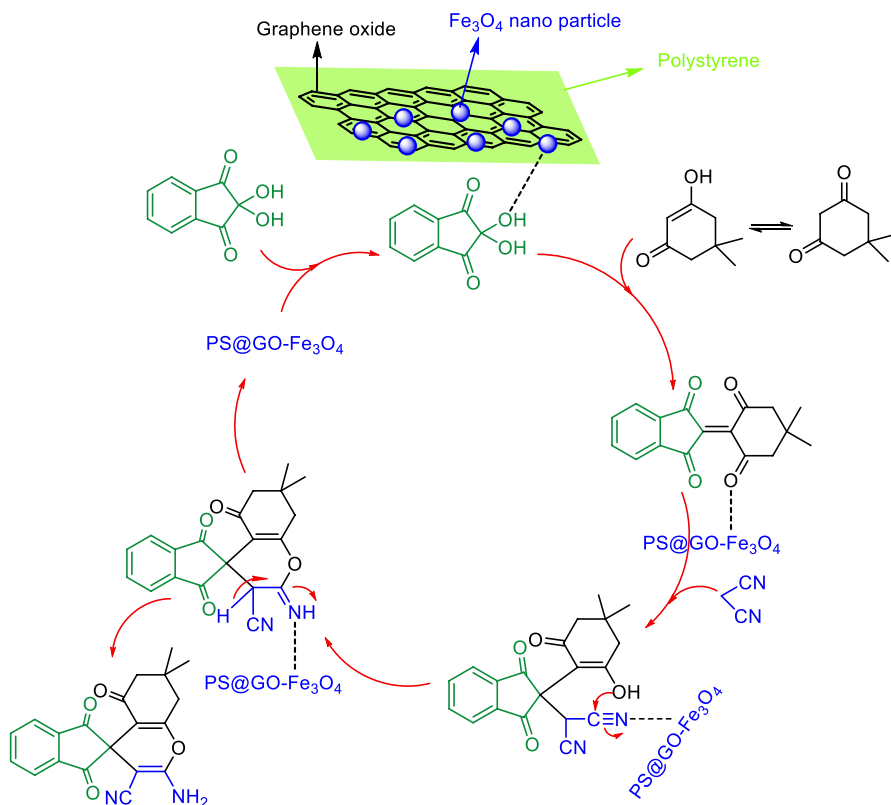


**Scheme 4** Four-component synthesis of 2'-amino-spiro[indeno[1,2-*b*]quinoxaline-11,4'-pyran]-3'-carbonitrile in the presence of PS@GO-Fe<sub>3</sub>O<sub>4</sub> nanocomposite

Finally, we compared the current study for the synthesis of 2'-amino-5',6',7',8'-tetrahydro-7',7'-dimethyl-5-oxospiro[indeno[1,2-*b*]quinoxaline-11,4'-[4'*H*]pyran]-3'-carbonitrile **7a** with other methods reported in the literatures (Table 4). The results clearly prove the preference of the present procedure.

## Conclusion

In conclusion, PS@GO-Fe<sub>3</sub>O<sub>4</sub> nanocomposite was prepared and characterized by FT-IR, TEM and VSM analyses. The catalytic activity of this nanocomposite was evaluated in the synthesis of two series of spiro indene and spiro indoline derivatives. It was found that this novel heterogeneous catalyst is an excellent choice for the synthesis of these biologically active heterocycles due to its efficiency, nontoxicity, thermal stability, mechanical stretch, low cost, simple manufacturing procedure, reusability, high surface area, nanosize and magnetic behavior. Furthermore, short reaction times, mild reaction conditions, easy workup procedure, high yields of products and magnetic separation of the catalyst are worthy benefits of this method.



**Scheme 5** Proposed mechanism for the synthesis of 2'-aminospiro[indeno-2,4'-pyran]-3'-carbonitriles in the presence of PS@GO-Fe<sub>3</sub>O<sub>4</sub> nanocomposite

**Table 3** Investigation of reusability of nanomagnetic PS@GO-Fe<sub>3</sub>O<sub>4</sub> in the model reaction

No. of runs	1	2	3	4	5	6	7	8
Yield (%) <sup>a</sup>	93	93	91	90	90	88	88	85

<sup>a</sup>Isolated yields after 2 h

**Table 4** Comparison of methods for the synthesis of 2'-amino-5',6',7',8'-tetrahydro-7',7'-dimethyl-5-oxospiro[indeno[1,2-*b*]quinoxaline-11,4'-[4'H]pyran]-3'-carbonitrile (**7a**)

Entry	Reaction conditions	Time (h)	Yield (%)
1	PS@GO-Fe <sub>3</sub> O <sub>4</sub> (10 mg) <sup>a</sup> , EtOH, reflux	2.5	85
2	InCl <sub>3</sub> (15 mol%), CH <sub>3</sub> CN, reflux [25]	11	91
3	AcONH <sub>4</sub> (20 mol%), EtOH, reflux [26]	12	91
4	Na <sub>2</sub> CO <sub>3</sub> (10 mol%), EtOH, reflux [27]	12	93
5	Et <sub>3</sub> N (2 equiv.), EtOH, reflux [28]	2	81

<sup>a</sup>1 mmol of all starting materials was used under optimized reaction conditions

**Acknowledgements** The authors thank Hakim Sabzevari University for the financial support of this work.

## References

1. M.J. Kukla, H.J. Breslin, C.J. Diamond, P.P. Grous, C.Y. Ho, M. Miranda, J.D. Rodgers, R.G. Sherrill, E. Clercq, R. Pauwels, *J. Med. Chem.* **34**, 3187 (1991)
2. J.T.C. Wojtyk, E. Buncel, P.M. Kazmaier, *Chem. Commun.* 1703 (1998)
3. B.M. Trost, *Science* **254**, 1471 (1991)
4. A. Hasaninejad, A. Zare, M. Shekouhy, J. Ameri Rad, *J. Comb. Chem.* **12**, 844 (2010)
5. A. Khazaei, M.A. Zolfigol, A.R. Moosavi-Zare, F. Abi, A. Zare, H. Kaveh, *Tetrahedron* **69**, 212 (2013)
6. A.R. Moosavi-Zare, M.A. Zolfigol, S. Farahmand, A. Zare, A.R. Pourali, R.J. Ayazi-Nasrabadi, *Synlett* **25**, 193 (2014)
7. A.R. Moosavi-Zare, M.A. Zolfigol, M.J. Daraei, *Synlett* **25**, 1173 (2014)
8. H.I. El-Subbagh, S.M. Abu-Zaid, M.A. Mahran, F.A. Badria, A.M. Al-Obaid, *J. Med. Chem.* **43**, 2915 (2000)
9. R. Hekmatshoar, S. Majedi, K. Bakhtiari, *Catal. Commun.* **9**, 307 (2008)
10. K. Singh, J. Singh, H. Singh, *Tetrahedron* **52**, 14273 (1996)
11. M. Darbarwar, V. Sundaramurthy, *Synthesis* 337 (1982)
12. T.-S. Jin, R.-Q. Zhao, T.-S. Li, *Arkivoc* **11**, 176 (2006)
13. M. Veverka, E. Krařoviřova, *Collect. Czechoslov. Chem. Commun.* **55**, 833 (1990)
14. A. Darehkordi, Z. Karimi-Taleghani, O.A. Pouralimardan, *J. Iran. Chem. Soc.* **11**, 623 (2014)
15. R.C. Gadwood, B.V. Kamdar, L.A.C. Dubray, M.L. Wolfe, M.P. Smith, W. Watt, *J. Med. Chem.* **36**, 1480 (1993)
16. M.M. Badran, A.A. Moneer, H.M. Refaat, A.A. El-Malah, *J. Chin. Chem. Soc.* **54**, 469 (2007)
17. R. Sarges, H.R. Howard, R.G. Browne, L.A. Lebel, P.A. Seymour, B.K. Koe, *J. Med. Chem.* **33**, 2240 (1990)
18. S.T. Hazeldine, L. Polin, J. Kushner, K. White, N.M. Bouregeois, B. Crantz, *J. Med. Chem.* **45**, 3130 (2002)
19. X. Li, L. Yang, Ch. Peng, X. Xie, H.-J. Leng, B. Wang, Zh-W Tang, G. He, L. Ouyang, W. Huang, B. Han, *Chem. Commun.* **49**, 8692 (2013)
20. X. Xie, L. Xiang, Ch. Peng, B. Han, *Chem. Rec.* **19**, 1 (2019)
21. A. Ding, M. Meazza, H. Guo, J.W. Yang, R. Rios, *Chem. Soc. Rev.* **47**, 5946 (2018)
22. X. Xie, W. Huang, Ch. Peng, B. Han, *Adv. Synth. Catal.* **360**, 194 (2018)
23. A. Korte, J. Legros, C. Bolm, *Synlett* 2397 (2004)
24. J.A. Makawana, M.P. Patel, R.G. Patel, *Arch. Pharm.* **345**, 314 (2012)
25. A. Hasaninejad, N. Golzar, A. Zare, *J. Heterocycl. Chem.* **50**, 608 (2013)
26. A. Hasaninejad, N. Golzar, M. Shekouhy, A. Zare, *Helvetica* **94**, 2289 (2011)
27. E. Soleimani, M. Hariri, P. Saei, *ChemistrySelect* **16**, 773 (2013)
28. F. Chen, J. Zheng, M. Huang, Y. Li, *Chem. Sci.* **41**, 5545 (2015)
29. X. Wu, P. Kiu, *Macromol. Res.* **18**, 1008 (2010)
30. R. Sengupta, M. Bhattacharya, S. Bandyopadhyay, A.K. Bhowmick, *Prog. Polym. Sci.* **36**, 638 (2011)
31. K.S. Kim, Y. Zhao, H. Jang, S.Y. Lee, J.M. Kim, K.S. Kim, J.H. Ahn, P. Kim, J.Y. Choi, B.H. Hong, *Nature* **457**, 706 (2009)
32. J.T. Robinson, F.K. Perkins, E.S. Snow, Z.Q. Wei, P.E. Sheehan, *Nano Lett.* **8**, 3137 (2008)
33. M.D. Stoller, S.J. Park, Y.W. Zhu, J.H. An, R.S. Ruff, *Nano Lett.* **8**, 3498 (2008)
34. G. Eda, G. Fanchini, M. Chhowalla, *Nat. Nanotechnol.* **3**, 270 (2008)
35. E. Yoo, J. Kim, E. Hosono, H. Zhou, T. Kudo, I. Honma, *Nano Lett.* **8**, 2277 (2008)
36. R. Muszynski, B. Seger, P.V. Kamat, *J. Phys. Chem. C* **112**, 5263 (2008)
37. B. Zahed, H. Hosseini-Monfared, *Appl. Surf. Sci.* **328**, 536 (2015)
38. Y. Li, Y. Cao, J. Xie, D. Jia, H. Qin, Z. Liang, *Catal. Commun.* **58**, 21 (2015)

39. N. Hashim, Z. Muda, M.Z. Hussein, I.M. Isa, A. Mohamed, A. Kamari, S.A. Bakar, M. Mamat, A.M. Jaafar, *J. Mater. Environ. Sci.* **7**, 3225 (2016)
40. F. Kim, L.J. Cote, J. Huang, *Adv. Mater.* **22**, 1954 (2010)
41. M.Z. Kasaei, E. Motamedi, M. Majidi, *Chem. Eng. J.* **172**, 540 (2011)
42. Ph Biehl, M. von der Lühe, S. Dutz, F.H. Schacher, *Polymers* **10**, 91 (2018)
43. S.F. Hojati, A.H. Amiri, N. MoeiniEghbali, S. Mohamadi, *Appl. Organomet. Chem.* **32**, e4235 (2018)
44. S.F. Hojati, A.H. Amiri, S. Mohamadi, N. MoeiniEghbali, *Res. Chem. Intermed.* **44**, 2275 (2018)
45. S.F. Hojati, A.H. Amiri, H. Raouf, *Appl. Organomet. Chem.* **31**, e3595 (2017)
46. S.F. Hojati, N. MoeiniEghbali, S. Mohamadi, T. Ghorbani, *Org. Prep. Proced. Int.* **50**, 408 (2018)
47. S.F. Hojati, M. Moosavifar, T. Ghorbanipoor, *CR Chem.* **20**, 520 (2017)
48. I. Mohammadpoor-Baltork, A.R. Khosropour, S.F. Hojati, *Catal. Commun.* **8**, 200 (2007)
49. I. Mohammadpoor-Baltork, A.R. Khosropour, S.F. Hojati, *Catal. Commun.* **8**, 1865 (2007)
50. D.C. Marcano, D.V. Kosynkin, J.M. Berlin, A. Sinitskii, Z. Sun, A. Slesarev, L.B. Alemany, W. Lu, J.M. Tour, *ACS Nano* **4**, 4806 (2010)
51. P. Saluja, K. Aggarwal, J.M. Khurana, *Synth. Commun.* **43**, 3239 (2013)
52. H.R. Safaei, M. Shekouhy, S. Rahmanpur, A. Shirinfeshan, *Green Chem.* **14**, 1696 (2012)
53. P. Nazari, A. Bazi, S.A. Ayatollahi, H. Dolati, S.M. Mahdavi, L. Rafighdoost, M. Amirmostofian, *Iran. J. Pharm. Res.* **16**, 943 (2017)
54. E. Soleimani, M. Hariri, P. Saei, *CR Chim.* **16**, 773 (2013)

**Publisher's Note** Springer Nature remains neutral with regard to jurisdictional claims in published maps and institutional affiliations.